*Supplement of*

# Spatiotemporal optimization of $NO_x$ and VOC emissions using a hybrid inversion framework and its implication for ozone sensitivity diagnosis

Jeonghyeok Moon[1], Wonbae Jeon[2,3], Sujong Jeong[4,5,6], Yunsoo Choi[7], Hyun Cheol Kim[8,9], Soon-Young Park[10], Juseon Bak[11], Jung-Woo Yoo[11], Jaehyeong Park[12], Dongjin Kim[2,12], Hyeonsik Choe[2,12], Chae-Yeong Yang[2,12], Min Heo[2,12]

[1]Environmental Planning Institute, Seoul National University, Seoul 08826, South Korea
[2]BK21 School of Earth and Environmental System, Pusan National University, Busan 46241, South Korea
[3]Department of Atmospheric Sciences, Pusan National University, Busan 46241, South Korea
[4]Department of Environmental Management, Graduate School of Environmental Studies, Seoul National University, Seoul, 08826, South Korea
[5]Climate Tech Center, Seoul National University, Seoul, 08826, South Korea
[6]Institute for Sustainable Development, Seoul National University, Seoul, 08826, South Korea
[7]Department of Earth and Atmospheric Sciences, University of Houston, Houston, TX 77204, USA
[8]Air Resources Laboratory, National Oceanic and Atmospheric Administration, College Park, MD, 20740, USA
[9]Cooperative Institute for Satellite Earth System Studies, University of Maryland, College Park, MD, 20742, USA
[10]Department of Science Education, Daegu National University of Education, Daegu, 42411, South Korea
[11]Institute of Environmental Studies, Pusan National University, Busan 46241, South Korea
[12]Division of Earth Environmental System, Pusan National University, Busan 46241, South Korea

*Correspondence to*: Wonbae Jeon (wbjeon@pusan.ac.kr)

**Table S1: Model configurations of the Weather Research and Forecasting (WRF) simulation.**

| WRF | Domain 01(D1) | Domain 02(D2) |
|---|---|---|
| Horizontal Resolution (Number of grids) | 27 km (150 × 135) | 9 km (79 × 79) |
| Vertical layers | 35 Layers | |
| Microphysics option | WSM 3-class simple ice scheme | |
| Radiation option | RRTM scheme(long-wave)<br>Dudhia scheme(short wave) | |
| Surface layer option | Revised MM5 Monin-Obukhov scheme (Jimenez) | |
| Land-surface option | Unified Noah land-surface model | |
| PBL option | YSU scheme | |
| Cumulus option | Kain-Fritsch (new Eta) scheme | |
| Initial data | ERA5 (0.25˚ × 0.25˚) | |
| Simulation period | 2022. 04. 26. 00 UTC – 2022. 05. 16. 00 UTC | |

**Table S2: Model configurations of the Community Multi-scale Air Quality (CMAQ) simulation.**

| CMAQ | Domain 01(D1) | Domain 02(D2) |
|---|---|---|
| Horizontal Resolution (Number of grids) | 27 km (137 × 122) | 9 km (66 × 66) |
| Vertical layers | 15 Layers | |
| Anthropogenic emission | EDGAR_HTAPv3 | |
| Biogenic emission | MEGANv2.1 | |
| Chemical mechanism | cb05cl_ae5_aq | |
| Simulation period | 2022. 04. 27. 00 UTC – 2022. 05. 15. 00 UTC | |

**Table S3: List of VOC species included in this study according to the carbon bond mechanism version 2005 (CB05).**

| Model species | Definition |
|---|---|
| ALD2 | Acetaldehyde |
| ALDX | Aldehydes with 3 or more carbons |
| ETH | Ethene |
| ETHA | Ethane |
| FORM | Formaldehyde |
| IOLE | Internal alkene bond |
| ISOP | Isoprene |
| MEOH | Methanol |
| NVOL | Non-volatile compounds |
| OLE | Terminal alkene bond |
| PAR | Carbon-carbon single bond |
| TERP | Monoterpenes |
| TOL | Toluene and other monoalkyl aromatics |
| UNR | Unreactive |
| XYL | Xylene |

**Table S4. Statistical metrics used for evaluating model performance and inverse modeling results. Here, $n$ is the total number of compared points, $O_i$ is the observed value or ideal emission value, and $M_i$ is the value of the CMAQ model value.**

| Descriptions | Metrics | Formula |
|---|---|---|
| Mean observation | $\bar{O}$ | $\frac{\sum_{i=1}^{n} O_i}{n}$ |
| Mean model | $\bar{M}$ | $\frac{\sum_{i=1}^{n} M_i}{n}$ |
| Mean bias error | MBE | $\frac{\sum_{i=1}^{n}(M_i - O_i)}{n}$ |
| Root mean square error | RMSE | $\sqrt{\frac{\sum_{i=1}^{n}(M_i - O_i)^2}{n}}$ |
| Index of agreement | IOA | $1 - \frac{\sum_{i=1}^{n}(M_i - O_i)^2}{\sum_{i=1}^{n}(\lvert M_i - \bar{O}\rvert + \lvert O_i - \bar{O}\rvert)^2}$ |
| Correlation coefficient | r | $\sum_{i=1}^{n}((\frac{O_i - \bar{O}}{\sqrt{\sum_{i=1}^{n}(O_i - \bar{O})^2}}) \times (\frac{M_i - \bar{M}}{\sqrt{\sum_{i=1}^{n}(M_i - \bar{M})^2}}))$ |
| Normalized mean error | NME | $\frac{\sum_{i=1}^{n}\lvert M_i - O_i\rvert}{\sum_{i=1}^{n} O_i} \times 100$ [%] |

**Table S5. Statistical evaluation of 2 m temperature, 2 m relative humidity, and 10 m wind speed from the WRF simulation. Observational data were obtained from ASOS stations.**

| | OBS | WRF | MBE | RMSE | IOA | r |
|---|---|---|---|---|---|---|
| Temperature [°C] | 16.03 | 14.88 | -1.16 | 2.35 | 0.94 | 0.91 |
| Wind speed [m $s^{-1}$] | 1.93 | 3.19 | 1.25 | 1.90 | 0.68 | 0.60 |
| Relative humidity [%] | 59.74 | 62.89 | 3.16 | 12.95 | 0.90 | 0.82 |

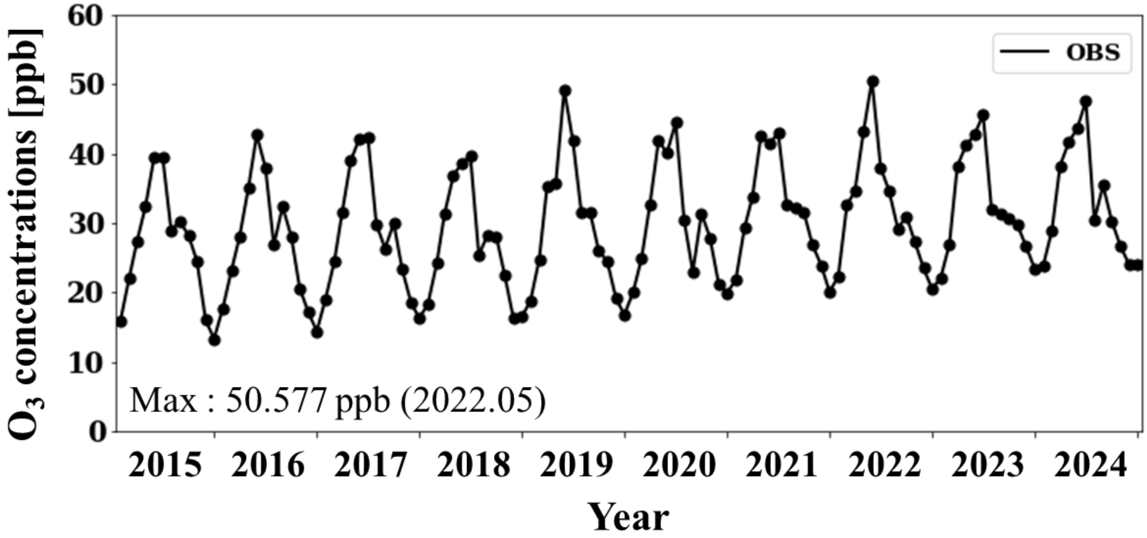


**Figure S1: Monthly averaged time series of observed $O_3$ concentrations over South Korea during the recent decade (2015–2024), based on the AQMS network.**

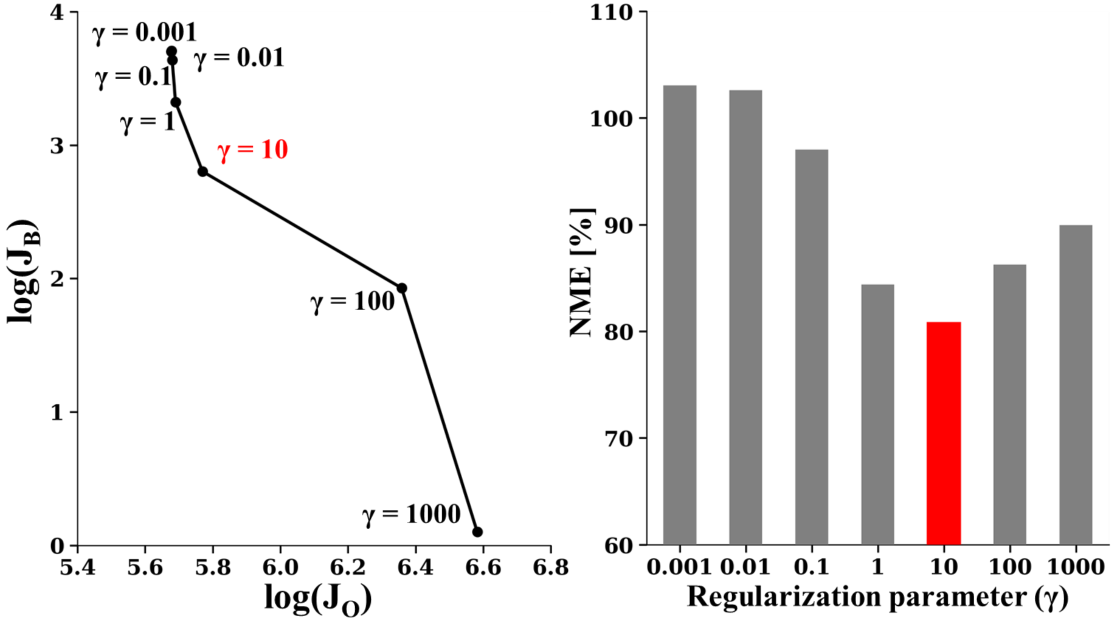


**Figure S2: Results of the L-curve test and emission NME [%] used to determine the optimal regularization parameter ($\gamma$) for the 4D-Var inverse modeling. The test was performed for $\gamma$ values of 0.001, 0.01, 0.1, 1, 10, 100, and 1000, based on the simulation for 1 May 2022.**

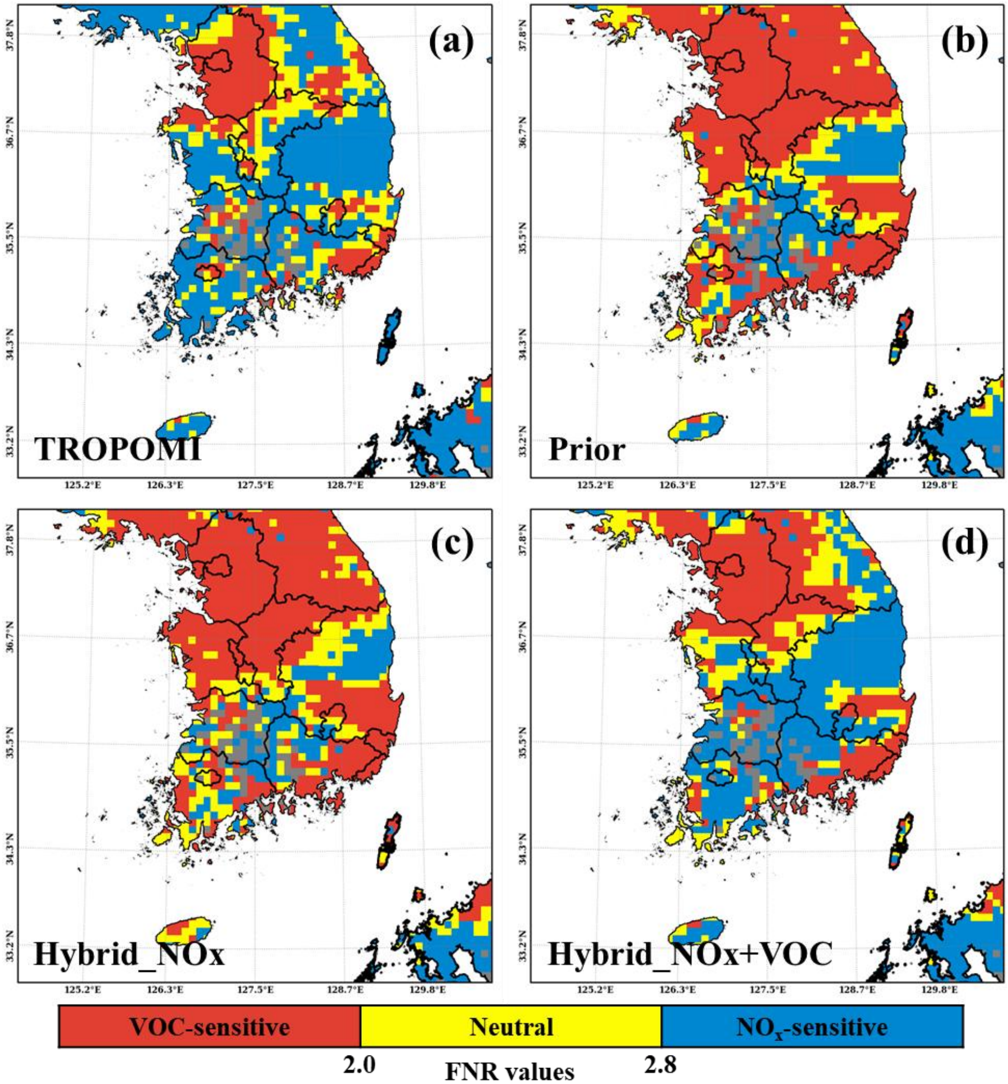


**Figure S3: Spatial distributions of $O_3$ sensitivity regimes for (a) TROPOMI-based FNR, (b) Prior, (c) Hybrid_NOx, and (d) Hybrid_NOx+VOC experiments, averaged over the study period. Red, yellow, and blue indicate VOC-sensitive, neutral, and $NO_x$-sensitive regimes, respectively. Gray areas denote missing data.**